# A THEORETICAL ANALYSIS OF THE EFFECTS OF SONICATION ON DIFFERENTIAL ABSORPTION FLATTENING IN SUSPENSIONS OF MEMBRANE SHEETS

C. L. TEETERS,* J. ECCLES,‡ AND B. A. WALLACE*
*Department of Biochemistry and Biophysics, Columbia University, New York, New York 10032; and
‡Department of Computer Services, City College of New York, New York, New York 10031

ABSTRACT A theoretical analysis is presented for the flattening of absorption and circular dichroic spectra of suspensions of membrane sheets containing proteins. Equations are presented to describe the dependence of this artifact on the size of the sheets. Values for the flattening coefficients $Q_A$ and $Q_B$ are calculated both as a function of absorptivity and sheet size. These studies show that sonication is an inadequate procedure for eliminating flattening in these samples.

## INTRODUCTION

Spectroscopic studies of membranes are influenced by the physical nature of such samples. It has been noted that the absorbance and circular dichroic (CD) spectra of membranes suffer from certain optical artifacts because of their particulate nature and that if these artifacts are not corrected for, the estimated protein secondary structures calculated from such spectra will be grossly in error (Urry, 1972; Schneider and Harmatz, 1976; Wallace and Mao, 1984). One such artifact is absorption flattening, which has the effect of nonlinearly attenuating intense absorption peaks and CD bands at strong absorption peaks.

Membrane proteins exist in a phospholipid environment that critically affects their secondary structure. Previous experimental methods attempting to alleviate absorption flattening have included solubilization in detergents. However, since there is considerable risk that the secondary structure will change when the samples are solubilized in detergent, it becomes important to measure the circular dichroic spectra of samples that better represent the in situ environment of the protein. Hence, alternate procedures have been used to reduce absorption flattening effects while retaining a membrane environment. These procedures include sonication of the membrane samples to minimize the size of the particles and incorporation of the protein into small unilamellar vesicles to both decrease the size of the particles and reduce the concentration of the protein within the lipid phase (Mao and Wallace, 1984; Nabedryk et al., 1985). We present here a theoretical analysis of how particle shape and size will affect the extent of absorption flattening of membrane sheets and predict the effect sonication will have on the CD spectra of membranes.

The absorption spectrum of a suspension of absorbing particles is flattened when compared with a homogeneous solution of the same species (Duysens, 1956). This is due solely to the colloidal nature of the material and introduces an artifact that must be separated from the intrinsic properties of the absorbing species. Flattening is a statistical phenomenon that occurs because the light going through the sample has a lessened probability of actually encountering the absorbing phase. The absorbance flattening by suspensions of solid cubes and spheres (Duysens, 1956) and of spherical shells (Gordon and Holzwarth, 1971) has been evaluated. Gordon and Holzwarth have also examined the flattening of circular dichroic spectra for suspensions of optically active particles of these shapes.

Here we determine the flattening caused by suspensions of flat sheets such as are formed by purple membrane. The analysis is first performed for sheets that have a large diameter relative to the membrane thickness. It is then extended to cases in which the size of the sheet is smaller, and the effects of particle size on the flattening of absorbance and CD spectra is examined.

## THEORY FOR LARGE SHEETS

For suspensions of biological membranes containing proteins, which are the absorbing species of interest, essentially all of the absorbing material is in the lipid or particle phase. The specific case of protein-containing membrane sheets such as purple membranes will be modeled as disks

Dr. C. L. Teeter's present address is The BOC Group, Technical Center, Murray Hill, NJ 07974.

Dr. J. Eccles' present address is Cap Gemini America, Cranford, NJ 07016.

Dr. B. A. Wallace's present address and address for correspondence is Department of Chemistry, Rensselaer Polytechnic Institute, Troy, NY 12180-3590.

of radius $R$ and thickness $\Delta$, where the radius is much larger than the thickness. For this phase we assume an absorptivity $\epsilon$, such that light traveling through phase $p$ along a length $l$ is attenuated according to

$$I = I_0 \exp(-\epsilon l), \tag{1}$$

where $\epsilon$ includes the effect of the concentration of the absorbing species within the particle. Consider such a suspension in which fraction $q$ of the volume is the particulate phase, and $(1 - q)$ is the solvent. The absorbance of the solution along a pathlength $h$ would be

$$A_{sol} = \epsilon qh \tag{2}$$

if the absorbing species was homogeneously distributed through the volume. It is $A_{sol}$ that is sought but not necessarily measured since this idealized situation can not normally be achieved under experimental conditions. Our description of $A_{sol}$ is slightly different from that given by Duysens or Gordon and Holzwarth but is equivalent.

The desired quantity $A_{sol}$ is related to the measured quantity $A_{sus}$, the absorbance of the suspension, by the equation

$$Q_A = \frac{A_{sus}}{A_{sol}}. \tag{3}$$

The particles have an area $\sigma_p$ normal to the incident light beam, and a volume $v_p$. The transmittance of a single particle is $T_p$, and the suspension contains $N$ such particles per unit volume. For a single particle suspended in the bulk solvent, the attenuation of the light going through a unit area of the sample, assuming this area completely includes the particle, is

$$\frac{I}{I_0} = (1 - \sigma_p) + \sigma_p T_p, \tag{4}$$

where the first term describes light that does not hit the particle, while the second term is the fraction of light hitting the particle that is not absorbed. The absorbance of this sample is

$$A_p = -\ln(I/I_0) = -\ln[1 - \sigma_p(1 - T_p)], \tag{5}$$

where for $\sigma_p(1 - T_p) \ll 1$ simplifies to:

$$A_p = \sigma_p(1 - T_p). \tag{6}$$

This assumption is acceptable when the volume fraction $q \ll 1$, which is true for most experimental samples.

If we look at a suspension with $N$ such particles per unit length, or total particles $M = Nh$, Eq. 4 is replaced by the summation

$$\frac{I}{I_0} = \sum_{i=0}^{M} [(1 - \sigma_{pi}) + \sigma_{pi} T_{pi}] \tag{7}$$

and Eq. 6 by

$$A_{sus} = \sum_{i=0}^{M} \sigma_{pi}(1 - T_{pi}). \tag{8}$$

In the cases examined by Duysens and by Gordon and Holzwarth, the particles were uniform and so

$$A_{sus} = Nh\,\sigma_p(1 - T_p). \tag{9}$$

This is true if there is negligible apparent overlap between particles as seen by the incident light, that is, for $q \ll 1$.

The phase fraction $q$ can be expressed as

$$q = Nv_p \tag{10}$$

for uniform particles where $v_p$ is the volume of one particle, and so from Eq. 2

$$A_{sol} = Nh\epsilon v_p. \tag{11}$$

The measure of absorption flattening for uniform isotropic particles is then

$$Q_A = \frac{A_{sus}}{A_{sol}} = \frac{[\sigma_p(1 - T_p)]}{\epsilon v_p}. \tag{12}$$

For nonuniform particles

$$Q_A = \frac{\sum_{i=0}^{M} [\sigma_{pi}(1 - T_{pi})]}{\epsilon \sum_{i=0}^{M} v_{pi}}. \tag{13}$$

It is immediately apparent from this form that although the absorbance flattening results from the colloidal nature of the suspension, there is no dependence on sample pathlength $h$ or fractional volume $q$. The value of $Q_A$ depends only on the properties of the particles, except when Eq. 2 and 6 break down for high values of $q$, when substantial amounts of overlap of particles can occur.

Gordon and Holzwarth define $Q_B$, which is the flattening of a CD spectrum

$$Q_B = \frac{\theta_{sus}}{\theta_{sol}} = \frac{(A_{sus}^{+} - A_{sus}^{-})}{(A_{sol}^{+} - A_{sol}^{-})} \approx \frac{dA_{sus}}{dA_{sol}}. \tag{14}$$

Here $A^+$ and $A^-$ are the absorbance of left and right circularly polarized light, respectively. The last approximation is acceptable since $\theta \ll A$.

From Eq. 13 all the information we need is in the quantities $v_p$, $\sigma_p$, and $T_p$. The volume $v_p$ is just

$$v_p = \pi R^2 \Delta. \tag{15}$$

The values of $\sigma_p$ and $T_p$, however, depend upon the orientation of the particle disk relative to the light beam. If the vector normal to the face of the disk makes an angle $\phi$ with the incident light beam, then

$$\sigma_p = \pi R^2 \cos\phi. \tag{16}$$

$T_p$ is the quantity $\exp(-\epsilon l)$ averaged over all paths through the particle. The light has to travel through a pathlength $l = \Delta/\cos\phi$ (assuming $\Delta \ll R$) and so

$$T_p = \exp(-\epsilon\Delta/\cos\phi). \tag{17}$$

The particles are not identical but rather are a collection with random orientation. We therefore apply Eq. 8, replacing the sum with the integrations over the continuum value d cos $\phi$ and the volume element d$\theta$, giving

$$A_{sus} = \frac{Nh \int_0^{2\pi} d\theta \int_0^1 \pi R^2 \cos\phi [1 - \exp(-\epsilon\Delta/\cos\phi)] d\cos\phi}{\int_0^{2\pi} d\theta \int_0^1 d\cos\phi} \quad (18)$$

which results in

$$A_{sus} = \frac{Nh\pi R^2}{2}\{1 - [(1 - \epsilon\Delta)\exp(-\epsilon\Delta) - \epsilon^2\Delta^2 Ei(-\epsilon\Delta)]\}, \quad (19)$$

where

$$Ei(-x) = -\int_x^\infty [\exp(-B)/B] dB. \quad (20)$$

The quantity $Q_A$ is now

$$\frac{A_{sus}}{A_{sol}} = \frac{Nh\pi R^2}{2Nh\epsilon\pi R^2\Delta} \cdot \{1 - [(1 - \epsilon\Delta)\exp(-\epsilon\Delta) - \epsilon^2\Delta^2 Ei(-\epsilon\Delta)]\}. \quad (21)$$

For ease of comparison with the results of Gordon and Holzwarth, we define an effective absorptivity $\alpha_p = A_{sol}/qm$, $m$ being the average number of particles per unit length of sample. For membrane sheets this quantity per particle is

$$\alpha_p = 2\epsilon\Delta \quad (22)$$

and so $Q_A$ becomes

$$Q_A = \frac{1}{\alpha^p} \cdot \{1 - [(1 - \alpha_p/2)\exp(-\alpha_p/2) - \frac{\alpha_p^2}{4} Ei(-\alpha_p/2)]\}, \quad (23)$$

which is the same as the results reported by Gordon and Holzwarth for a spherical shell. The only difference is that the absorptivity per particle $\alpha_p$ is dependent upon the geometrical shape of the particle and has a value $4\epsilon\Delta$ for a spherical shell. The apparent thickness of a spherical shell is just twice that of the apparent thickness of a sheet, since the light passes through two sides of the hollow sphere.

For circular dichroism, the model for membrane sheets gives

$$Q_B = \exp(-\alpha_p/2) + \frac{\alpha_p}{2} Ei(-\alpha_p/2), \quad (24)$$

which is also the same as the spherical shell case except for the form of $\alpha_p$.

An experimental example of membrane sheets can be found in purple membrane (PM) patches. These samples are single bilayers of ~55 Å thick and a dimension of 0.5–1.0 $\mu$m. Circular dichroism studies have shown significant absorption flattening of the spectrum of large PM sheets compared with the predicted spectrum based on the secondary structure of bacteriorhodopsin obtained from x-ray data (Mao and Wallace, 1984; Wallace and Teeters, 1987). From these data, it was estimated that $Q_B$ for these large sheets is 0.45 at 193 nm and 0.6 at 224 nm.

Alternatively, using decadic molar residue extinction coefficients of $1.1 \times 10^4$ and $2.44 \times 10^3$ at 193 and 224 nm, respectively, calculated from Wetlaufer (1962), one can roughly estimate $\alpha_p$ for PMs without resorting to knowledge about the protein structure. Assuming that the protein density is 1.4 g/ml and that the lipids occupy ~25% of the purple membrane, the residue molar concentration of bacteriorhodopsin in PMs will be ~11. Therefore, $\alpha_p$ will equal $2 \times 2.3 \times 1.1 \times 10^4 \times 11 \times 55 \times 10^{-7}$ or 0.31 at 193 nm and 0.068 at 224 nm. From Fig. 2, the corresponding values of $Q_B$ are 0.63 and 0.87, respectively. These values are somewhat larger than those estimated above from the experimental data. However, in nonpolar environments, the extinction coefficients of aromatic amino acids can increase up to twofold relative to their values in aqueous environments. Since such amino acids may be buried in the hydrophobic core in PMs, this would mean that this calculation would tend to underestimate $\alpha_p$ or overestimate $Q_B$. If this environmental factor were taken into account, the values calculated in this way could approach the experimental values for $Q_B$. In either case, it can be seen that the flattening coefficient values for these samples estimated either by experiment or calculation are significant at all wavelenths in the far UV.

## THEORY FOR A MODERATE-SIZED SHEET

By analogy to Eq. 8, the absorbance of a uniform suspension of particles, which can vary continuously in some property $u$, is given by

$$A_{sus} = hN \int \sigma_p(1 - T_p)\, du, \quad (25)$$

where the integral ranges over all allowed values of $u$. The value $T_p$ is simply an average of $\exp(-\epsilon l)$ over the projection of the surface area of the particle onto the plane perpendicular to the incident light. That is

$$T_p = \frac{\int_{\sigma_p} \exp[-\epsilon l(s)]\, ds}{\int_{\sigma_p} ds} = \frac{1}{\sigma_p}\int_{\sigma_p} \exp[-\epsilon l(s)]\, ds. \quad (26)$$

For the present case the membrane patch is modeled as a square block, $2R$ on a side, and thickness $\Delta$. Such a particle has a volume $v_p = 4R^2\Delta$. For simplicity, the sheet is assumed to always have one edge perpendicular to the incident light. The implications of the choice of shape and the freezing of one degree of freedom are discussed later.

Again the angle between the vector normal to the face of the particle and the incident light is $\phi$.

The two-dimensional integral over the area coordinate $s$ is written in terms of coordinates $x$ and $y$, which are chosen as follows: both $x$ and $y$ are perpendicular to the incident light, and in addition, $x$ is along the edge of the sheet, which is constrained to be perpendicular to the light. So,

$$T_p = \frac{1}{\sigma_p}\int_0^{2R}\int_0^{y'''} \exp\left[-\epsilon l(y)\right] dy dx = \frac{2R}{\sigma_p}\int_0^{y'''} \exp\left[-\epsilon l(y)\right] dy, \quad (27)$$

where $y''' = 2R\cos\phi + \Delta\sin\phi$, and where

$$\sigma_p = \int_0^{2R}\int_0^{y'''} dy dx = 2R(2R\cos\phi + \Delta\sin\phi). \quad (28)$$

To proceed further, we note that two cases must be separately considered: $\phi < \phi_c$ and $\phi > \phi_c$ where $\tan\phi_c = 2R/\Delta = \gamma$. For either case there is a value of $y \equiv y'$ such that for $0 < y < y'$ light exits a surface perpendicular to the one it enters. For this range, the pathlength is $l(y) = y(\tan\phi + \cot\phi)$. There is also a second value $y \equiv y'' = y''' - y'$ such that for $y'' < y < y'''$ the same expression for $l(y)$ holds. For $y' < y < y''$, $l(y) = y'(\tan\phi + \cot\phi)$, and is constant. Note that for $\phi < \phi_c$, this constant pathlength is $\Delta/\cos\phi$, while for $\phi > \phi_c$, it is $2R/\sin\phi$. Using these pathlengths, we get:

$$T_p(\phi) = \frac{2R}{\sigma_p}\left\{2\int_0^{y'} \exp\left[-\epsilon y(\tan\phi + \cot\phi)\right] dy + (y'' - y')\exp\left[-\epsilon y'(\tan\phi + \cot\phi)\right]\right\}. \quad (29)$$

For $\phi < \phi_c$,

$$T_p(\phi) = \frac{1}{(\gamma\cos\phi + \sin\phi)}\left\{\frac{(4\sin\phi\cos\phi)}{\alpha_p}\left[1 - \exp\left(-\alpha_p/2\cos\phi\right)\right] + (\gamma\cos\phi - \sin\phi)\exp\left(-\alpha_p/2\cos\phi\right)\right\} \quad (30)$$

and for $\phi > \phi_c$

$$T_p(\phi) = \frac{1}{(\gamma\cos\phi + \sin\phi)}\left\{\frac{(4\sin\phi\cos\phi)}{p}\left[1 - \exp\left(-\alpha_p\gamma/2\sin\phi\right)\right] - (\gamma\cos\phi - \sin\phi)\exp\left(-\alpha_p\gamma/2\sin\phi\right)\right\}. \quad (31)$$

This can be used to form $A_{sus}$.

$$A_{sus} = hN\int_0^1 \sigma_p(1 - T_p)\,d\cos\phi, \quad (32)$$

where

$$\sigma_p = 4R^2\cos\phi + 2R\Delta\sin\phi = \Delta^2(\gamma^2\cos\phi + \gamma\sin\phi). \quad (33)$$

Also, from Eq. 11

$$A_{sol} = hN\epsilon v_p = hN\epsilon 4R^2\Delta = \frac{hN\Delta^2\gamma^2\alpha_p}{2} \quad (34)$$

giving

$$Q_A = \frac{A_{sus}}{A_{sol}} = \frac{2}{\alpha_p\gamma}\int_0^1 (\gamma\cos\phi + \sin\phi)(1 - T_p)\,d\cos\phi. \quad (35)$$

While this could be solved in closed form, it is a simple matter to perform the integration numerically on a computer.

The expression for circular dichroism is rewritten as

$$Q_B = \frac{d\,A_{sus}}{d\,A_{sol}} = \frac{d(Q_A A_{sol})}{dA_{sol}} = \frac{d(\alpha_p Q_A)}{d\alpha_p}. \quad (36)$$

Again we have performed the derivative numerically.

Eqs. 35 and 36 allow us to examine the behavior of $Q_A$ and $Q_B$ as a function of the size of the particle. There are only two parameters involved in determining these values. The first is $\alpha_p = 2\epsilon\Delta$. We assume that $\Delta$ remains fixed, which would be true for membranes. The value of $\alpha_p$ therefore is proportional to $\epsilon$, which varies only with wavelength. The second parameter is $\gamma = 2R/\Delta$, which varies with $R$ and thus would change on sonication of membrane patches. The results of the calculations for various $\alpha_p$ and $\gamma$ are given in Figs. 1–4.

Figs. 1 and 2 show $Q_A$ and $Q_B$, respectively, as a function

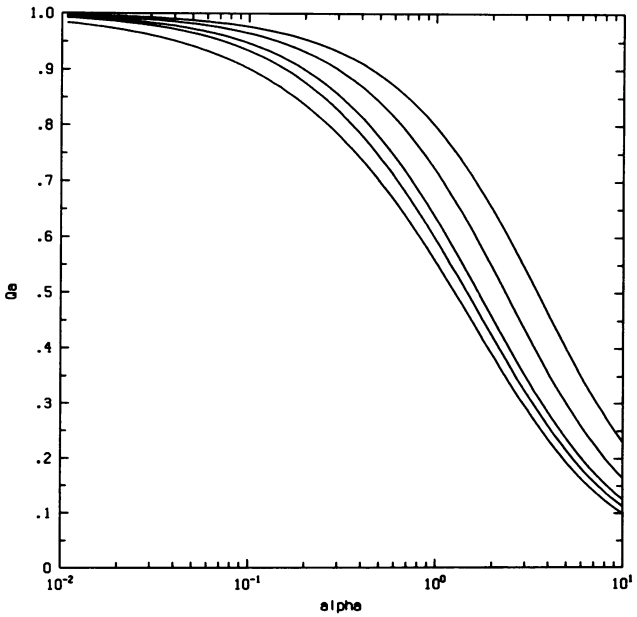


FIGURE 1 The dependence of $Q_A$ for membrane sheets on the absorptivity per particle $\alpha_p$. Individual curves, from top to bottom, represent the different values of $\gamma = 1, 2, 5, 10$, and $\infty$, where $\infty$ symbolizes the limit $R \gg \Delta$.

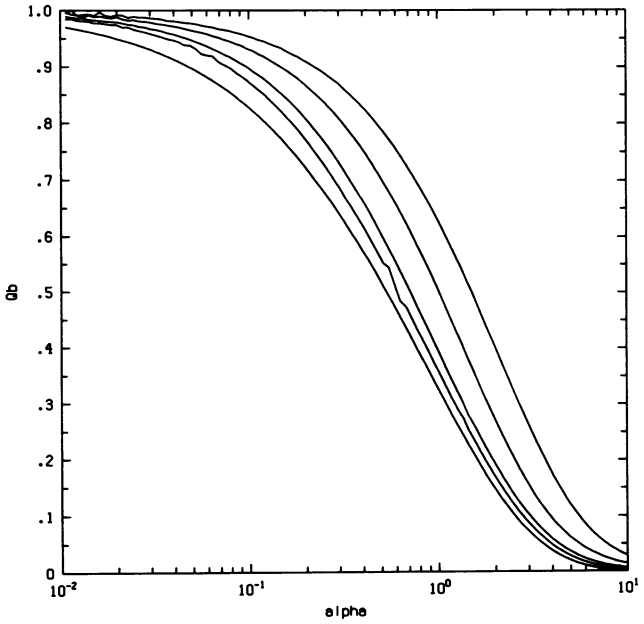


FIGURE 2 The dependence of $Q_B$ for membrane sheets on the absorptivity per particle $\alpha_p$. Individual curves, from top to bottom, represent the different values of $\gamma = 1, 2, 5, 10$, and $\infty$, where $\infty$ symbolizes the limit $R \gg \Delta$.

of $\alpha_p$ for values of $\gamma = 1, 2, 5, 10$, and $\infty$ (that is the limiting case $R \gg \Delta$). The irregularities seen on the graphs for $Q_B$ are artifacts resulting from the numerical differentiation in its calculation. The large sheet limit corresponds to the greatest absorbance flattening. Sonication of the membrane sheets can be expected to alleviate some of this effect, but not a great amount.

The effect of the changes that may be observed can be seen clearly in Figs. 3 and 4, which show $Q_A$ and $Q_B$ vs. $\gamma$ for selected values of $\alpha_p$. They are almost independent of $\gamma$ beyond ~10, and in fact the decrease in absorbance flattening even at $\gamma = 5$ is not large. This value of $\gamma = 5$ represents the approximate limit to which sonication can break up membrane patches.

Purple membranes can also be used as a test case for the effects of sonication. Sonication produces membrane patches of the same thickness (55 Å) but of a diameter of ~250 Å or larger, and increases the experimentally-measured values of $Q_B$ to 0.54 and 0.64 at 193 and 224 nm, respectively. As can be seen from Fig. 2, if $Q_B$ is taken as 0.45 and 0.6 from the experimental values for intact sheets, then it will be 0.54 and 0.69 for $\gamma = 5$. Our results therefore agree to within experimental error.

## DISCUSSION

A few words should be said about some of the simplifying assumptions made to obtain Eqs. 35 and 36 and the behavior of these equations in some limiting cases. In the case of $R \gg \Delta$ Eqs. 35 and 36 become identical to Eqs. 23 and 24, respectively, for circular sheets. This is to be expected since the only geometric parameter that affects $Q_A$ and $Q_B$ in this limit is the thickness, which enters the derivation as $v_p/\sigma_p = \Delta/\cos\phi$. In this limit the two models give identical results that are independent of $R$.

As shown in the Theory for a moderate-sized sheet section, this independence fails as $R$ approaches the size of $\Delta$. In the limiting case of $\gamma = 1$ one would expect the results to approach those for a cube of side $\Delta$. In comparison with

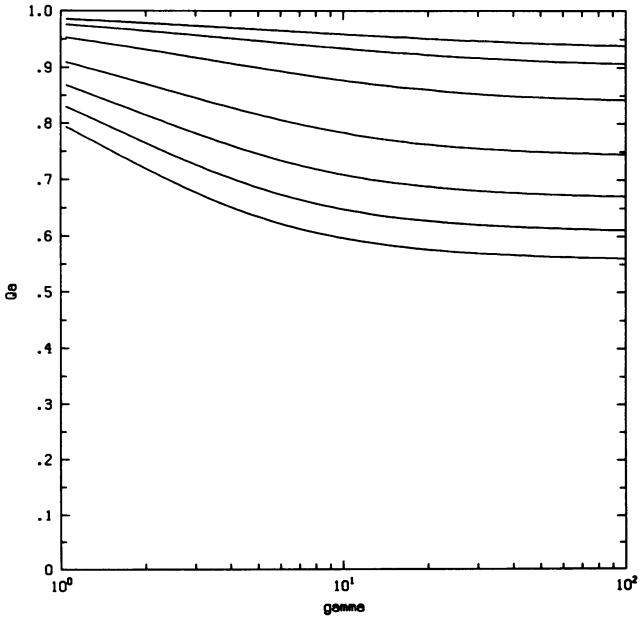


FIGURE 3 The dependence of $Q_A$ for membrane sheets on the quantity $\gamma = 2R/\Delta$, which is a measure of the size of the sheet. Individual curves, from top to bottom, represent the different values of $\alpha_p = 0.06, 0.1, 0.2, 0.4, 0.6, 0.8$, and 1.0.

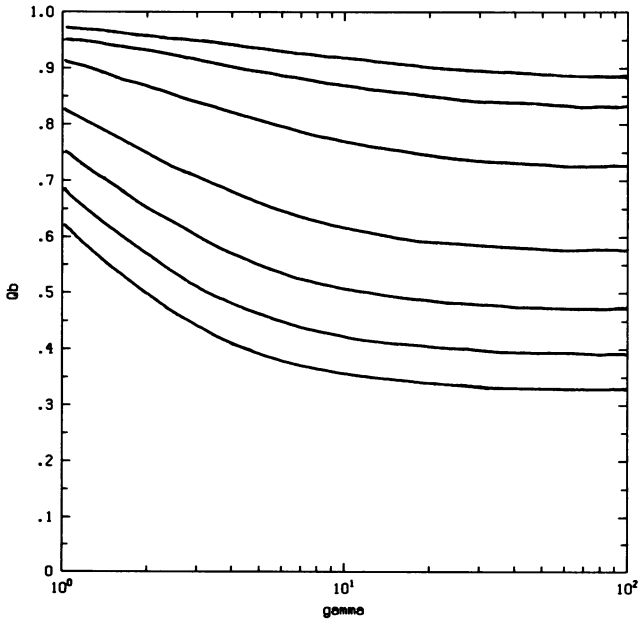


FIGURE 4 The dependence of $Q_B$ for membrane sheets on the quantity $\gamma = 2R/\Delta$, which is a measure of the size of the sheet. Individual curves, from top to bottom, represent the different values of $\alpha_p = 0.06, 0.1, 0.2, 0.4, 0.6, 0.8$, and 1.0.

the values of $Q_A$ and $Q_B$ as derived by Gordon and Holzwarth, one can not simply take equal values of $A_{sol}/qm$. A careful examination shows that their equations for the case of a cube with sides of length $d$ in terms of $\alpha_p = 2\epsilon d$ are

$$Q_A = (2/\alpha_p)[1 - \exp(-\alpha_p/2)] \quad (37)$$

and

$$Q_B = \exp(-\alpha_p/2). \quad (38)$$

These equations generate results very similar to our expression for $\gamma = 1$. The choice of the form for $\alpha_p$ reflects the difference in effective pathlength due to the averaging over orientation in the case of sheets.

In summary, we have extended the work of Gordon and Holzworth (1971) on absorption flattening to include the case of membrane sheets, and have shown the dependence of flattening on the size of the particles. These calculations have also shown that sonication will have a negligible effect on the flattening properties of membranes and that it cannot be used to eliminate the effect of an uneven distribution of chromophores in optical measurements.

During the course of these studies, B. A. Wallace was the recipient of a Dreyfus Teacher-Scholar Award.

This work was supported by National Institutes of Health grants GM-27292 and AM-3108.

## REFERENCES

Duysens, L. N. M. 1956. The flattening of absorption spectrum of suspensions compared to that of solutions. *Biochim. Biophys. Acta.* 19:1–12.

Gordon, D. J., and G. Holzwarth. 1971. Artifacts in the measured optical activity of membrane suspensions. *Arch. Biochem. Biophys.* 142:481–488.

Nabedryk, E., A. M. Bardin, and J. Breton. 1985. Further characterization of protein secondary structure in purple membrane by circular dichroism and polarized infrared spectroscopies. *Biophys. J.* 48:873–876.

Mao, D., and B. A. Wallace. 1984. Differential light scattering and absorption flattening effects are minimal in the circular dichroism spectra of small unilamellar vesicles. *Biochemistry.* 23:2667–2673.

Schneider, A. S., and D. Harmatz. 1976. An experimental method correcting for absorption flattening and scattering in suspensions of absorbing particles: circular dichroism spectra of hemoglobin in situ in red blood cells. *Biochemistry.* 15:4158–4162.

Urry, D. W. 1972. Protein conformation in biomembranes: optical rotation and absorption of membrane suspensions. *Biochim. Biophys. Acta.* 265:115–168.

Wallace, B. A., and D. Mao. 1984. Circular dichroism analyses of membrane proteins: an examination of light scattering and absorption flattening in large membrane vesicles and membrane sheets. *Anal. Biochem.* 142:317–328.

Wallace, B. A., and C. L. Teeters. 1987. Differential absorption flattening optical effects are significant in the circular dichroism spectra of large membrane fragments. *Biochemistry.* In press.

Wetlaufer, D. B. 1962. Ultraviolet spectra of proteins and amino acids. *Adv. Protein Chem.* 17:303–390.